

An Efficient Tree for the LIBOR Market Model

Hsi-Kang Hsu

摘要

LIBOR 市場模型 (LMM) 是一種廣泛用於定價利率衍生品的利率模型。然而，定價衍生品需要將所有利率帶到同一機率度量下進行。這種轉換使利率不再呈對數正態分佈並引入了複雜的狀態相依漂移，因此為 LMM 建構一個高效樹模型變得非常具有挑戰性。本論文提出了用於單因子、常數波動率 LMM 的高效率樹狀模型。我們的演算法為每個 LIBOR 利率構建了一個節點重合的三元樹。此三元樹可準確的計算出利率上限、利率下限和界限期權的價格。

關鍵字：三元樹、LMM 模型、樹狀模型、利率上限、利率下限、界限期權

Abstract

The LIBOR Market Model (LMM) is a widely used interest rate model for pricing interest rate derivatives. However, pricing derivatives requires bringing all forward rates under the same measure. This introduces a complex state-dependent drift. Consequently, constructing an efficient tree for the LMM becomes challenging. This thesis presents an efficient tree for the single-factor, constant-volatility LMM. Our algorithm constructs a recombining trinomial tree for each forward LIBOR rate. The proposed tree yields accurate prices for caplets, floorlets and barrier options.

Keywords: trinomial tree, LIBOR market model, lattice model, caplet, floorlet, barrier option

Contents

	Page
摘要	i
Abstract	iii
Contents	v
List of Figures	vii
List of Tables	ix
Chapter 1 Introduction	1
Chapter 2 Preliminaries	5
2.1 The LIBOR Market Model (LMM)	5
2.1.1 The LIBOR Rate Process	6
2.1.2 Terminal Measure	6
2.2 Interest Rate Derivatives	7
2.2.1 Caplets and Floorlets	7
2.2.2 Caps and Floors	8
2.2.3 Discrete Barrier Caps/Floors	8
Chapter 3 Numerical Results	11
3.1 Numerical Analysis of the Convergence in Mean and Variance	11
3.2 Valuation of Caplets/Floorlets in the LMM	19

3.3	Valuation of Discrete Barrier Options in the LMM	25
Chapter 4	Conclusion	27
References		29

List of Figures

3.1	Probability-weighted relative errors for the means of the tree nodes for $\ln L_1$ with 10 times steps.	14
3.2	Probability-weighted relative errors for the means of the tree nodes for $\ln L_1$ with 25 times steps.	14
3.3	Probability-weighted relative errors for the means of the tree nodes for $\ln L_1$ with 50 times steps.	15
3.4	Probability-weighted relative errors for the variances of the tree nodes for $\ln L_1$ with 10 times steps.	15
3.5	Probability-weighted relative errors for the variances of the tree nodes for $\ln L_1$ with 25 times steps.	16
3.6	Probability-weighted relative errors for the variances of the tree nodes for $\ln L_1$ with 50 times steps.	16
3.7	Histogram of L_1 at its reset date generated by our trinomial tree with 50 steps and the Monte Carlo simulation of 100,000 samples.	17
3.8	Probability-weighted relative errors for the means of the tree nodes for $\ln L_9$ with 450 times steps.	17
3.9	Probability-weighted relative errors for the variances of the tree nodes for $\ln L_9$ with 450 times steps.	18
3.10	Relative errors of caplet prices with maturity 0.5 and volatility 10% against the strike rate.	22
3.11	Relative errors of floorlet prices with maturity 0.5 and volatility 10% against the strike rate.	22

3.12	Relative errors of caplet prices with maturity 4.5 and volatility 10% against the strike rate.	23
3.13	Relative errors of floorlet prices with maturity 4.5 and volatility 10% against the strike rate.	23
3.14	Relative errors of caplet prices with maturity 5 and volatility 10% against the strike rate.	24
3.15	Relative errors of floorlet prices with maturity 5 and volatility 10% against the strike rate.	24
3.16	Valuation of an up-and-out discrete barrier option with strike rate 4% and barrier rate 5%. The dashed lines denote the bounds of the 99.99% confidence interval generated by the Monte Carlo simulation.	26

List of Tables

3.1	Valuation of caplets with strike rate 4.7% and volatility 10% for different maturities. The longest-dated tree $\ln L_{10}$ has 500 time steps	20
3.2	Valuation of caplets with strike rate 4.7% and volatility 20% for different maturities. The longest-dated tree $\ln L_{10}$ has 500 time steps	20
3.3	Valuation of floorlets with strike rate 4.7% and volatility 10% for different maturities. The longest-dated tree $\ln L_{10}$ has 500 time steps	21
3.4	Valuation of floorlets with strike rate 4.7% and volatility 20% for different maturities. The longest-dated tree $\ln L_{10}$ has 500 time steps	21

Chapter 1 Introduction

The LIBOR market model (LMM) ([Brace, Gatarek, & Musiela, 1997](#)) is a financial model for interest rates. It models a set of forward LIBOR rates which can be observed in the market instead of the unobservable short rates or instantaneous forward rates. The LMM can be used to price various interest rate derivatives, from basic derivatives such as caplets and floorlets, to exotic derivatives such as swaptions.

The LMM models each forward LIBOR rate as a lognormal process under its respective forward probability measure. Change of measure can be applied so that all forward LIBOR rates are modeled under a common measure. This allows us to price derivatives that depend on multiple forward rates. However, the forward LIBOR rates would no longer be lognormal under the common measure. Therefore the pricing of derivatives would require numerical methods, such as Monte Carlo simulation or tree methods.

A few trees have been proposed for the LMM. Tang and Lange ([2001](#)) present non-exploding bushy trees for the multifactor LMM, which is essentially a subsampling of a conventional bushy tree. This technique allows the tree to grow over 100 time steps. Jaeckel ([2002](#)) proposes an general $(m + 1)$ -nomial non-recombining tree for the m -factor LMM. With the use of the alternating simplex direction method in conjunction with optimal simplex alignment, it produces convergent results for European swaptions for as little as 5

time steps. For example, a 4-factor model would require a tree of size $(4 + 1)^5 = 3125$. Dai, Chung and C. Ho (2009) adapt the methodology of T. Ho, Stapleton, and Subrahmanyam (1995) to construct a recombining binomial tree for the LMM, which has size quadratic in the number of time steps.

This thesis proposes an efficient tree for the LMM. It constructs a recombining trinomial tree for each forward LIBOR rate. We can then price derivatives using forward induction or backward induction.

Over the past few years, there has been increasing criticism surrounding the LIBOR and other IBOR rates due to market manipulation scandals and their failure to meet the RFR (risk-free rate) standards set by central banks and governments (Gyntelberg & Wooldridge, 2008). Consequently, governments in major economies have taken on the task of finding alternative RFRs. As explained by Lyashenko and Mercurio (2019):

By now, RFRs have been selected in all major economies: The US selected a new Treasuries repo financing rate called SOFR (Secured Overnight Funding Rate); the UK selected the reformed SONIA (Sterling Overnight Index Average); Switzerland selected SARON (Swiss Average Rate Overnight); Japan selected TONA (Tokyo Overnight Average Rate); and the Euro zone selected a new unsecured overnight rate called ESTER (Euro Short-Term Rate).

Progress on the global transition to RFRs in derivatives markets as of the end of 2022 is reported as follows (ISDA, 2023a):

By the end of 2022, almost 100% of OTC and ETD [exchange-traded derivatives] trading activity denominated in Japanese yen, sterling and Swiss franc

(as measured by DV01 [dollar duration]) referenced the corresponding RFRs.

The percentage of trading activity referencing SOFR increased from 28.4% of total US dollar IRD [interest rate derivative] DV01 in January 2022 to 64.1% in December 2022. The percentage of trading activity in the Euro Short-Term Rate (€STR) grew from 14.6% of total euro IRD DV01 in January 2022 to 22.0% in December 2022, as market participants continue to use EURIBOR along with €STR [ESTER].

Above, DV01 is used as the RFR adoption indicator, which was launched by the International Swaps and Derivatives Association in 2020 ([ISDA, 2020](#)). Statistics of OTC interest rate derivatives traded notional referencing RFRs as of the end of 2022 are summarized by the International Swaps and Derivatives Association as follows ([ISDA, 2023b](#)):

- OTC IRD traded notional referencing SOFR grew to \$54.5 trillion in 2022 versus \$9.4 trillion in 2021. SOFR transactions accounted for 38.5% of US dollar-denominated OTC IRD traded notional compared to 7.4% in 2021.
- IRD traded notional referencing SONIA rose to \$23.8 trillion in 2022 compared to \$20.6 trillion in 2021. SONIA-linked transactions represented 97.1% of sterling-denominated OTC IRD traded notional compared to 65.9% in 2021.
- €STR-linked OTC IRD traded notional increased to \$34.1 trillion in 2022 compared to \$3.0 billion in 2021. €STR-linked transactions comprised 36.0% of euro-denominated OTC IRD traded notional compared to 6.3% in 2021.

Since all the selected RFRs are overnight rates, in order for them to be used as replacements for IBORs, they first need to be converted into term rates, which are rates for various tenors, e.g., 1-month, 3-month and 6-month tenors. For this reason, SOFR has the SOFR Term Rate, SONIA has the Term SONIA Reference Rate, and TONA has the Tokyo Term Risk Free Rate (TORF). The quotes for these term RFRs use the same convention as the LIBORs. Thus the LMM can be applied to these term RFRs.

This thesis is organized as follows. The basic terms and preliminaries are reviewed in Chapter 2. Chapter 3 illustrates the construction of the proposed trinomial tree. Numerical results for caplets, floorlets and discrete barrier options are presented in Chapter 4. Chapter 5 concludes.

Chapter 2 Preliminaries

2.1 The LIBOR Market Model (LMM)

Denote $P(t, T)$ as the time t price of the zero-coupon bond with maturity T . The interest rate earned over a time period Δt is quoted as a LIBOR rate L . That is, one would earn the interest $\Delta t L$ at the end of the period Δt . This gives us the relation $1 = (1 + \Delta t L)P(0, \Delta t)$

The forward LIBOR rate $L_{T_1, T_2}(t)$ is the interest rate one can contract for at time t for the time period $[T_1, T_2]$. As the forward LIBOR rate $L_{T_1, T_2}(t)$ satisfies

$$P(t, T_1) = P(t, T_2)[1 + (T_2 - T_1)L_{T_1, T_2}(t)],$$

it can be written as

$$L_{T_1, T_2}(t) = \frac{1}{T_2 - T_1} \left[\frac{P(t, T_1) - P(t, T_2)}{P(t, T_2)} \right]. \quad (2.1)$$

The time T_2 here is known as the **maturity** for the forward LIBOR rate L_{T_1, T_2} and $T_2 - T_1$ is the **tenor**. $L_{T_1, T_2}(t)$ becomes the spot rate when $t = T_1$.

2.1.1 The LIBOR Rate Process

Assume there are n forward LIBOR rates $L_{T_{i-1}, T_i}(t)$, where $T_i - T_{i-1} = \alpha$ for some fixed tenor α and all $i = 1, 2, \dots, n$ with $T_0 = 0$. A fixed tenor for all forward LIBOR rates is assumed since in most markets, only forward LIBOR rates of one specific tenor is actively traded, which is usually three of six months.

Let $L_i(t)$ stand for $L_{T_{i-1}, T_i}(t)$. By the relation (2.1), the forward LIBOR rate $L_i(t)$ is the ratio of assets $P(t, T_{i-1}) - P(t, T_i)$ and $P(t, T_i)$ times a constant $1/\alpha$. If we take the zero-coupon bond $P(t, T_i)$ as the numeraire, $L_i(t)$ is a martingale under the T_i -forward probability measure $\mathbb{Q}(T_i)$ associated with $P(t, T_i)$ (Harrison & Kreps, 1979).

The LMM models the n forward LIBOR rates with the following stochastic differential equations (SDEs)

$$dL_i(t) = \sigma_i(t) L_i(t) dW^i, \quad (2.2)$$

where W^i denotes a Brownian motion under the T_i -forward probability measure $\mathbb{Q}(T_i)$ and σ_i is the deterministic volatility function of L_i . Equation (2.2) has the solution

$$L_i(t) = L_i(0) \exp \left\{ -\frac{1}{2} \int_0^t \sigma_i^2(s) ds + \int_0^t \sigma_i(s) dW^i(s) \right\}.$$

2.1.2 Terminal Measure

We can bring all forward LIBOR rates $L_i(t)$ under the same terminal measure $\mathbb{Q}(T_n)$. By using change of measure iteratively, we have

$$dL_i(t) = \left[- \sum_{k=i+1}^n \frac{\alpha L_k(t)}{1 + \alpha L_k(t)} \sigma_k(t) \sigma_i(t) \right] L_i(t) dt + \sigma_i(t) L_i(t) dW^n, \quad (2.3)$$

for all $i = 1, 2, \dots, n$ with the convention $\sum_{k=n+1}^n (\dots) = 0$.

By SDE (2.3), the forward LIBOR rates L_1, L_2, \dots, L_{n-1} are no longer martingales under the measure $\mathbb{Q}(T_n)$. Each has a drift term that depends on all forward LIBOR rates with a later maturity. As the SDE (2.3) is complicated, we can no longer solve it analytically but instead have to rely on numerical methods such as Monte Carlo simulation or lattice methods.

2.2 Interest Rate Derivatives

2.2.1 Caplets and Floorlets

A caplet is a call option on a forward LIBOR rate. Denote c_i as the caplet on L_i having cap rate K , then c_i pays $\alpha \cdot \max(L_i(T_{i-1}) - K, 0)$ at time T_i . Since L_i is a martingale under the T_i -forward probability measure $\mathbb{Q}(T_i)$, this caplet's price at time t can be written as

$$c_i(t) = \alpha P(t, T_i) \mathbb{E}_t^{\mathbb{Q}(T_i)} [\max(L_i(T_{i-1}) - K, 0)],$$

where $\mathbb{E}_t^{\mathbb{Q}(T_i)}$ denotes the conditional expectation under the measure $\mathbb{Q}(T_i)$.

This caplet's value at time t has the Black-like formula ([Black, 1976](#)) :

$$c_i(t) = \alpha P(t, T_i) \left[L_i(t) N(x) - K N(x - \sigma_i \sqrt{T_{i-1} - t}) \right],$$

where $N(\cdot)$ is the CDF of the standard normal distribution and

$$x \equiv \frac{\ln[L_i(t)/K] + (\sigma_i^2/2)(T_{i-1} - t)}{\sigma_i \sqrt{T_{i-1} - t}},$$

$$\sigma_i \equiv \sqrt{\frac{\int_t^{T_{i-1}} \sigma_i(s)^2 ds}{T_i - t}}.$$

Similarly, the floorlet is a put option on a forward LIBOR rate. The floorlet f_i on L_i having floor rate K pays $\alpha \cdot \max(K - L_i(T_{i-1}), 0)$ at time T_i . It's cost at time t also has the Black-like formula

$$f_i(t) = \alpha P(t, T_i) \left[K N(-x + \sigma_i \sqrt{T_{i-1} - t}) - L_i(t) N(-x) \right].$$

2.2.2 Caps and Floors

An interest cap makes payments at dates T_1, T_2, \dots, T_n with reset dates T_0, T_1, \dots, T_{n-1} . That is, the interest rate cap pays $\alpha \cdot \max(L_i(T_{i-1}) - K, 0)$ at each payment day T_i . This shows that a cap, which involves multiple forward LIBOR rates L_i , can be priced by summing up the individual caplet's price. Therefore caps do not require all L_i 's to be under the same measure to be priced.

Floors are defined analogously as paying $\alpha \cdot \max(K - L_i(T_{i-1}), 0)$ at each payment day T_i and can be priced by summing up the individual floorlet's price.

2.2.3 Discrete Barrier Caps/Floors

A discrete barrier cap/floor is a cap/floor with discrete monitoring dates, whose payoff is dependent on whether the underlying forward LIBOR rates breach the barrier level on those dates (Pelsser, 2000). Each caplet c_i in the barrier cap has a cap rate K_i and a barrier level H_i . The barrier condition is checked when the forward LIBOR rate L_i is reset.

To price a down-and-out barrier cap, which is a cap that terminates when the first L_i falls below the barrier level H_i at T_{i-1} , we decompose it into a series of down-and-out barrier caplets, just like what we did with caps. At time T_i , the i th barrier caplet has the payoff

$$\alpha \cdot \max(L_i(T_{i-1}) - K, 0) \cdot \prod_{k=1}^i \mathbb{1}(L_k(T_{k-1}) > H_k).$$

Above, $\mathbb{1}(\cdot)$ is the indicator function. The value of the down-and-out barrier cap can then be priced by summing up the individual down-and-out caplet's price. Clearly, the i th barrier caplet has a payoff that depends on not only L_i but also L_1, L_2, \dots, L_{i-1} . Hence all forward LIBOR rates must be brought under a single probability measure in pricing.

Chapter 3 Numerical Results

3.1 Numerical Analysis of the Convergence in Mean and Variance

Our trinomial tree does not match mean and variance exactly at each node except those on the tree for $\ln L_n$. In this section, we define the true mean and variance of each tree node and show numerically that both probability-weighted relative errors for the mean and variance of each tree node decrease as Δt decreases.

For the i th tree, recall the mean of node (u, v) for $\ln L_i$ is $\mu_i(u, v) \sigma_i$, where $\mu_i(u, v)$ is defined in (??). The variance of each node for $\ln L_i$ is σ_i^2 . The annualized mean and variance of each node (u, v) on the tree for $\ln L_i$ are, respectively,

$$\tilde{\mu}_i(u, v) \sigma_i = \Delta t^{-1} [p_u \cdot u_{u,v}^{(i)} + p_m \cdot m_{u,v}^{(i)} + p_d \cdot b_{u,v}^{(i)}],$$

$$\tilde{\sigma}_i^2(u, v) = \Delta t^{-1} [p_u \cdot (u_{u,v}^{(i)})^2 + p_m \cdot (m_{u,v}^{(i)})^2 + p_d \cdot (b_{u,v}^{(i)})^2] - [\tilde{\mu}_i(u, v) \tilde{\sigma}_i]^2.$$

The relative errors for the mean and variance of node (u, v) are defined, respectively, as $[\tilde{\mu}_i(u, v) - \mu_i(u, v)]/\mu_i(u, v)$ and $[\tilde{\sigma}_i^2(u, v) - \sigma_i^2]/\sigma_i^2$ and the probability-weighted relative error of mean and variance is the relative error times the probability of reaching node (u, v) .

We use the following setup from Pelsser (2000). The short rate curve is given by $Z(T) = 0.08 - 0.05 \exp \{-0.18T\}$. The prices of the zero-coupon bonds at time 0 are thus given by $P(0, T_i) = \exp \{-Z(T_i) T_i\}$. The tenor α is a constant and equals 0.5, therefore the LIBOR reset dates are given by $T_i = 0.5i$. We assume a flat volatility $\sigma_i = 10\%$ for all L_i and set $\sigma_{UB} = \sigma_i \sqrt{1.5}$.

We model ten LIBOR rates L_1, L_2, \dots, L_{10} . Figures 3.1–3.3 plot the probability-weighted relative errors for the means of the tree nodes for $\ln L_1$ with different numbers of time steps. Observe that all the surfaces share the same pattern. Figures 3.4–3.6 plot the probability-weighted relative errors for the variances of the tree nodes for $\ln L_1$ with different numbers of time steps. Again, all the surfaces share the same pattern. Both probability-weighted relative errors for the means and variances are concentrated on nodes close to the spine of the tree, i.e., nodes $(u, 0)$. The errors also increase along the spine of the tree towards the maturity.

The average probability-weighted relative errors for the means of the nodes in Figures 3.1–3.3 are 0.0022%, 0.0013%, and 0.0007%, respectively. The average probability-weighted relative errors for the variances of the nodes in Figures 3.4–3.6 are -0.0104% , -0.0054% , and -0.0027% , respectively. This shows that the average probability-weighted relative errors for both the means and the variances of the nodes decreases as the number of time steps increases. It is also clear from the figures that the largest probability-weighted relative error decreases as the number of time steps increases. Specifically, the largest probability-weighted relative error for the means of the nodes in Figures 3.1–3.3 are 0.0106%, 0.0079%, and 0.0056%, respectively. The largest probability-weighted relative error in absolute value for the variances of the nodes in Figures 3.4–3.6 are -0.0362% , -0.0269% , and -0.0193% , respectively. We conclude that increasing the number of time

steps (equivalently, decreasing Δt) decreases the probability-weighted relative errors of nodes on the tree uniformly.

Figure 3.7 compares the histogram of the LIBOR rate L_1 at its reset date generated by our trinomial tree to the histogram generated by the Monte Carlo simulation of 100,000 samples. The figure shows that the two distributions are similar. This explains why the probability-weighted relative errors for the means and variances are small.

We analyzed L_1 as its tree is likely to have the largest errors in mean and variance among trees for the forward LIBOR rates L_1, L_2, \dots, L_{10} . Recall from (??) that its drift $\mu_1(u, v) \sigma_1$ depends on those for L_2, L_3, \dots, L_{10} as well as those rates themselves, thus potentially adding up their individual errors, while the drift for $\ln L_9, \mu_9(u, v) \sigma_9$, depends on only the drift for L_{10} as well as L_{10} itself. To confirm this intuition, Figures 3.8 and 3.9 plot the probability-weighted relative errors for the means and variances of the tree nodes for $\ln L_9$, respectively. The Δt used in the tree for $\ln L_9$ is the same as those used in Figures 3.3 and 3.6 for fair comparison. Observe that both share the same patterns as those for L_1 . The average probability-weighted relative errors for the means and variances are 0.0001% and -0.0003% , respectively. The largest probability-weighted relative errors for the means and variances of the nodes are 0.0032% and -0.0077% , respectively. This shows that the tree for $\ln L_9$ incurs lower errors in mean and variance than those for $\ln L_1$.¹

¹Recall that the average probability-weighted relative errors for the means and variances of $\ln L_1$ are 0.0007% and -0.0027% , respectively. The largest probability-weighted relative errors for the means and variances of $\ln L_1$ are 0.0056% and -0.0193% , respectively

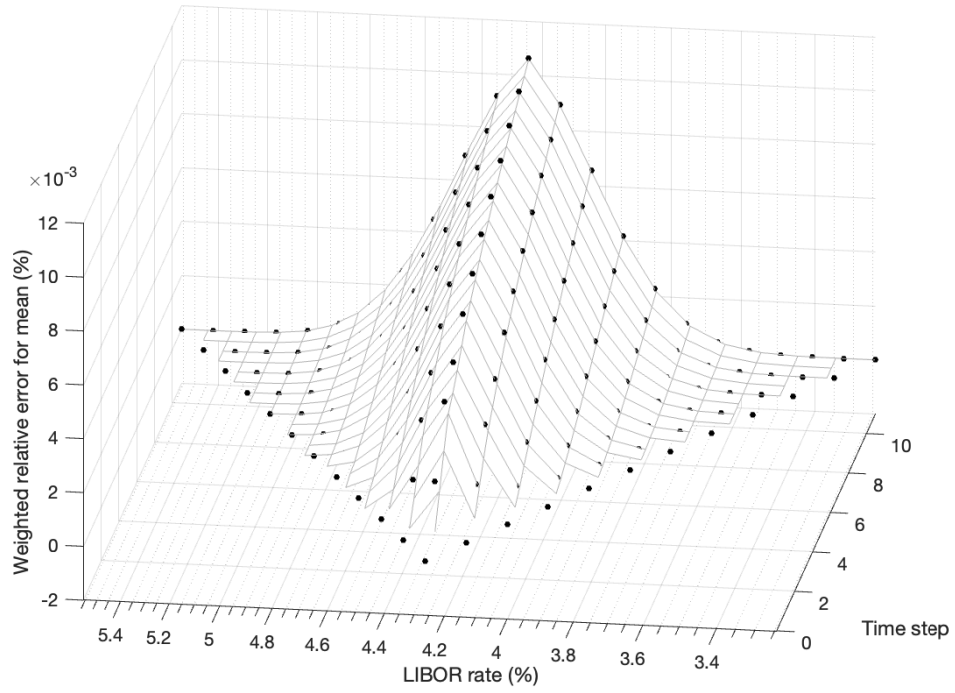


Figure 3.1: Probability-weighted relative errors for the means of the tree nodes for $\ln L_1$ with 10 times steps.

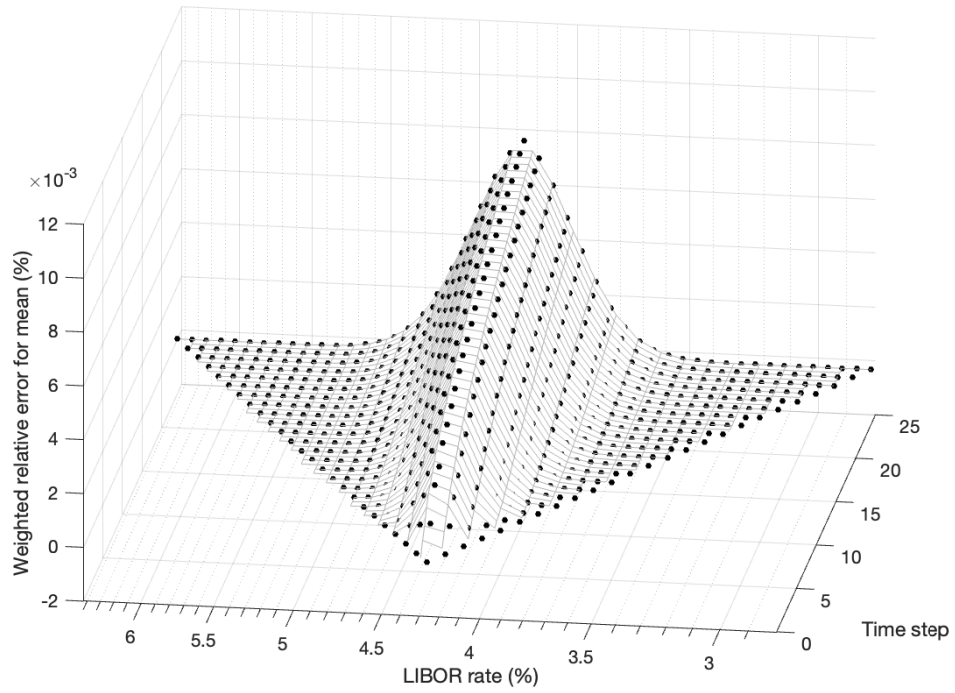


Figure 3.2: Probability-weighted relative errors for the means of the tree nodes for $\ln L_1$ with 25 times steps.

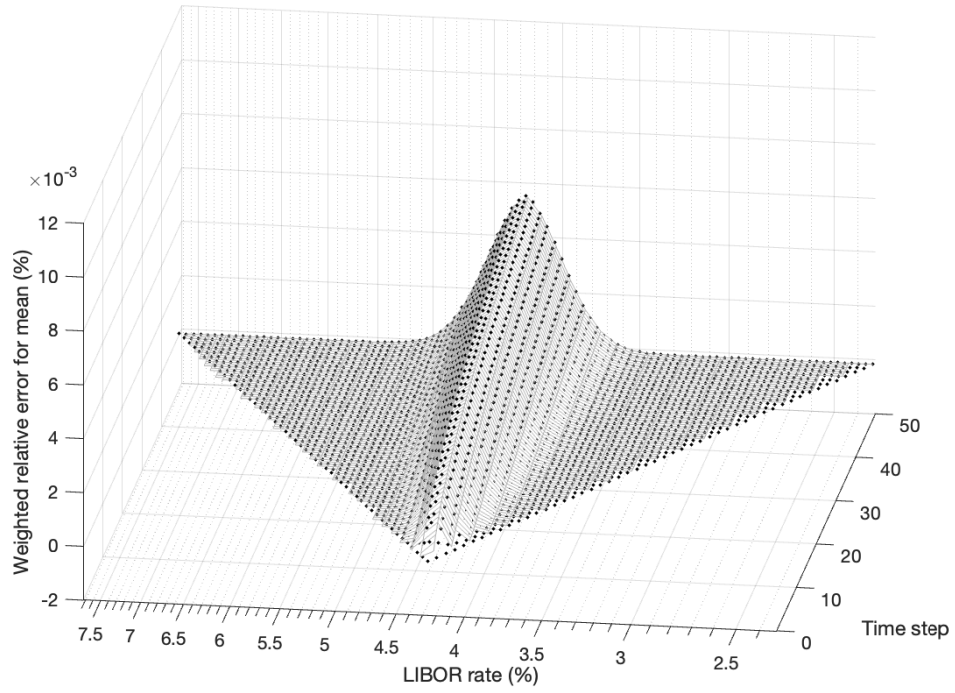


Figure 3.3: Probability-weighted relative errors for the means of the tree nodes for $\ln L_1$ with 50 times steps.

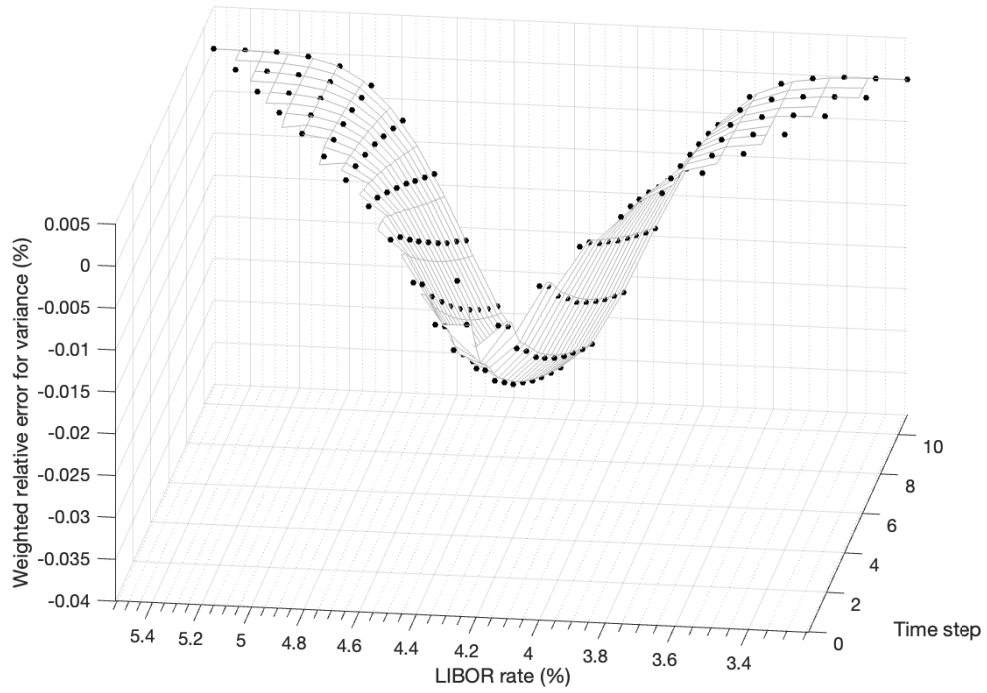


Figure 3.4: Probability-weighted relative errors for the variances of the tree nodes for $\ln L_1$ with 10 times steps.

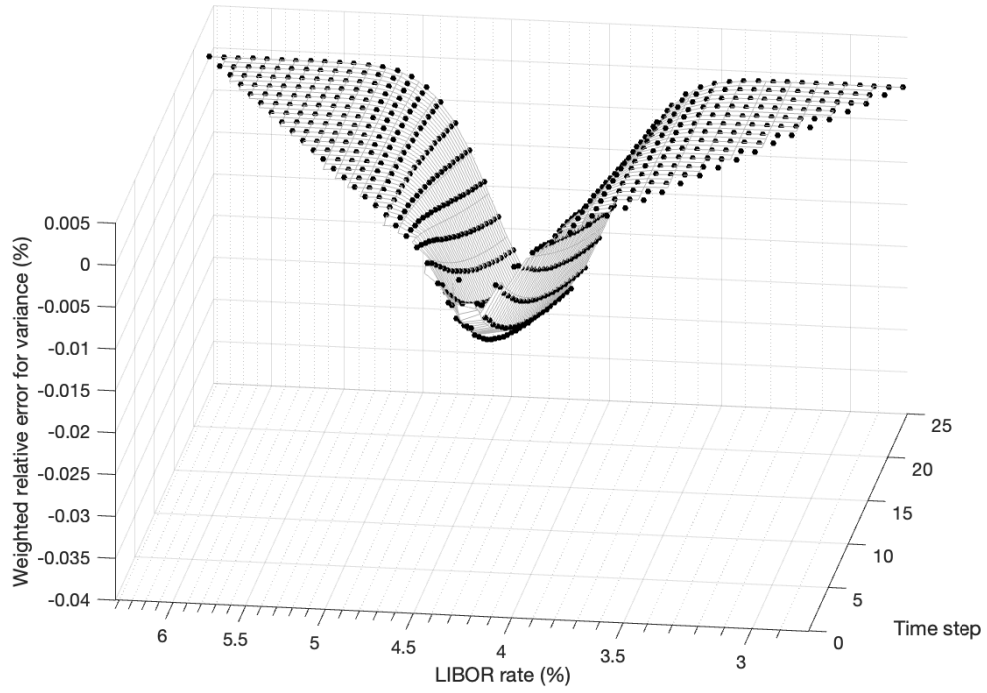


Figure 3.5: Probability-weighted relative errors for the variances of the tree nodes for $\ln L_1$ with 25 times steps.

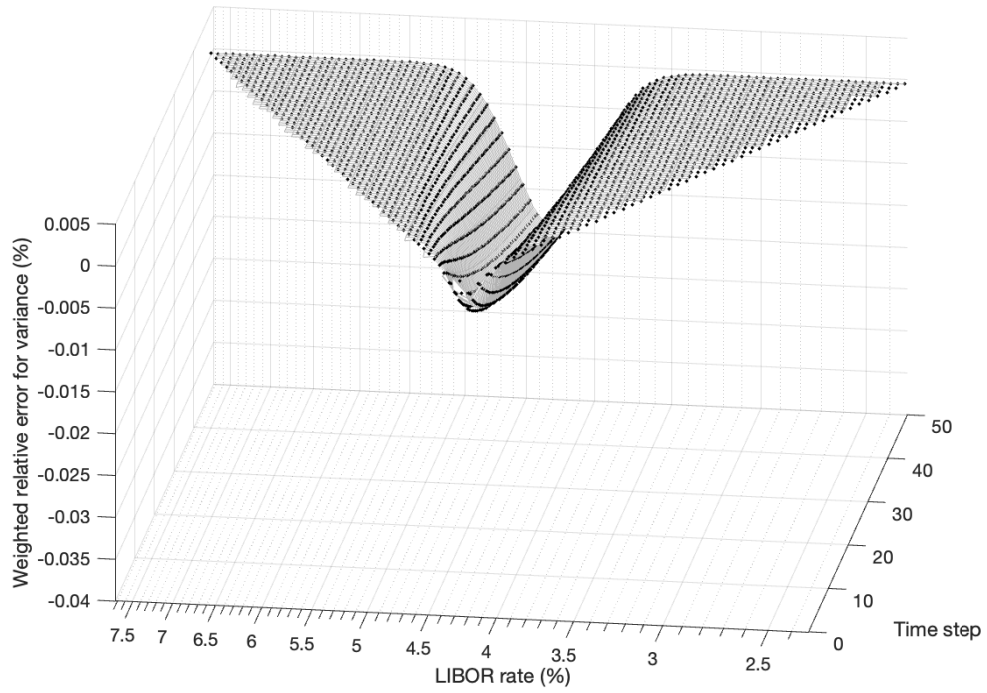


Figure 3.6: Probability-weighted relative errors for the variances of the tree nodes for $\ln L_1$ with 50 times steps.

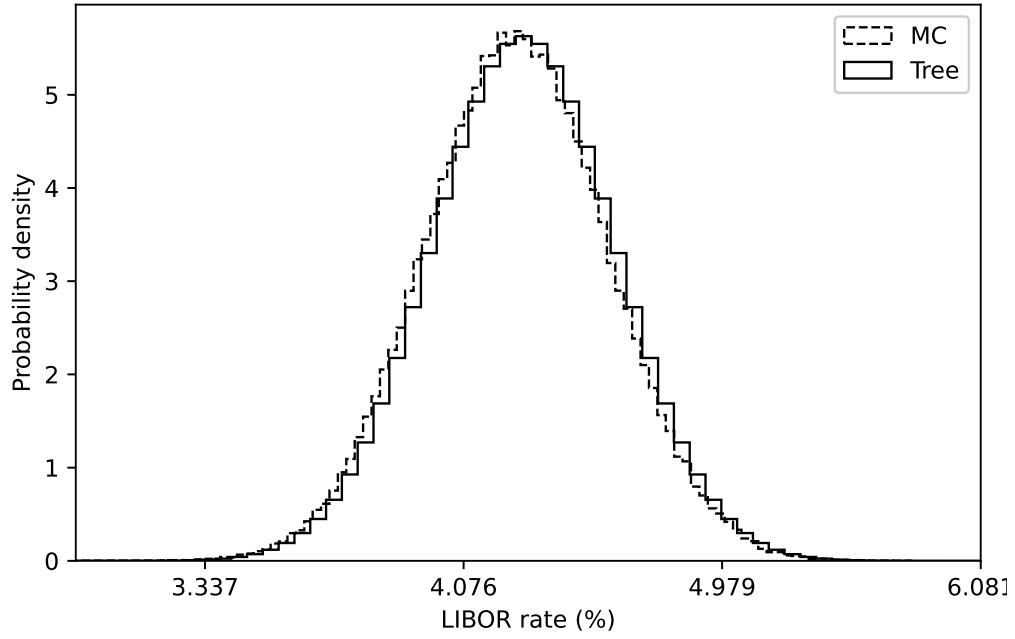


Figure 3.7: Histogram of L_1 at its reset date generated by our trinomial tree with 50 steps and the Monte Carlo simulation of 100,000 samples.

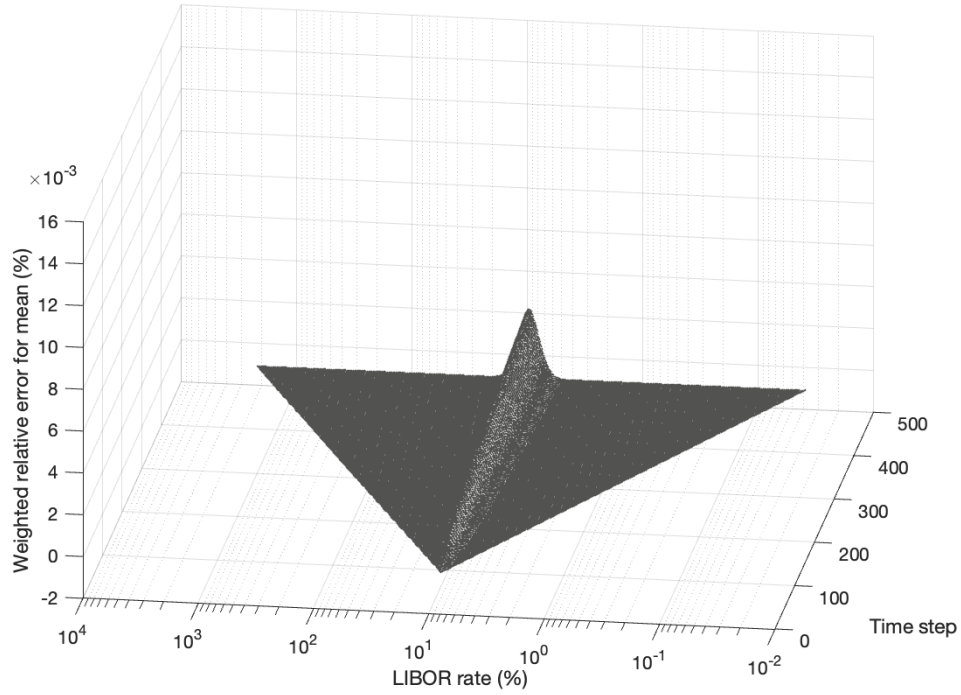


Figure 3.8: Probability-weighted relative errors for the means of the tree nodes for $\ln L_9$ with 450 times steps.

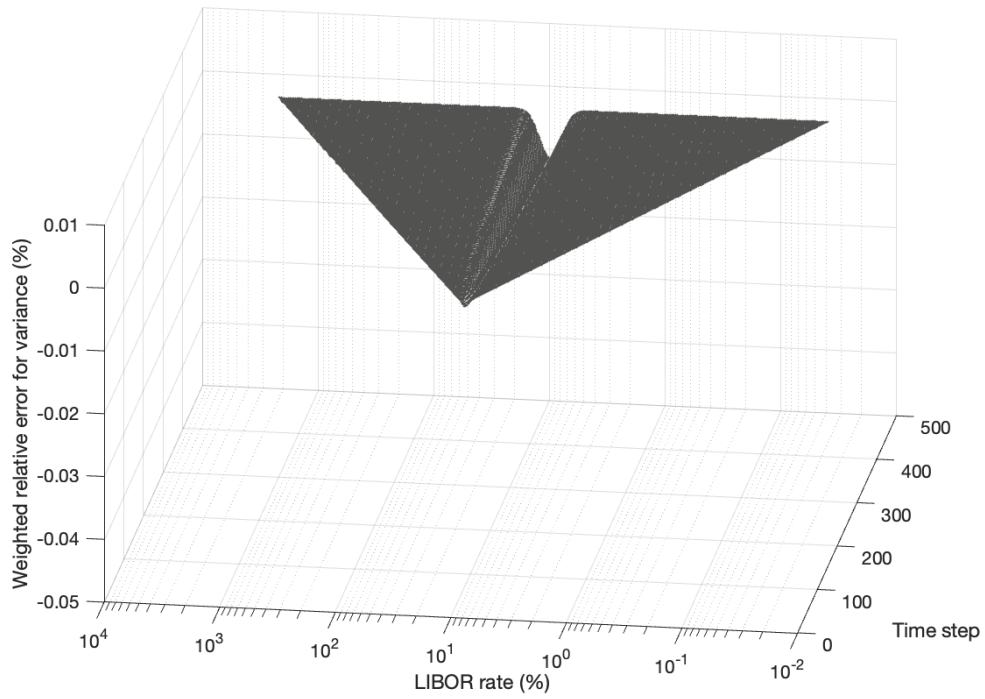


Figure 3.9: Probability-weighted relative errors for the variances of the tree nodes for $\ln L_9$ with 450 times steps.

3.2 Valuation of Caplets/Floorlets in the LMM

This section prices caplets and floorlets with our trinomial tree and compares them to the prices calculated by the Black-like formula. The setup used in this section are identical to those of Section 3.1.

Table 3.1 shows that the relative differences of the caplet prices from the Black formula lie within 0.66% for maturities up to 5 years. Increasing the volatility to 20% results in both higher and lower relative differences compared to the 10% case, but the relative differences remain very small, at below 0.66% (see Table 3.2). Table 3.3 shows that the relative differences of the floorlet prices from the Black formula lie within 1.9%. Increasing the volatility to 20% results in both higher and lower relative differences compared to the 10% case, but the relative differences remain very small, at below 1.7% (see Table 3.4). Note that our tree underprices the caplets and floorlets in Tables 3.1–3.4.

Figures 3.10–3.11 show that more time steps tend to lead to smaller relative errors when pricing caplets and floorlets. In particular, Figure 3.10 shows that 150 time steps is sufficient for the relative errors of the prices of caplets with a maturity of 0.5 year to stay within 4% over a broad range of strike rates. Similar results hold for floorlets as shown in Figure 3.11. Again, 150 time steps is sufficient for the relative errors of the prices of floorlets with a maturity of 0.5 year to stay within 5% over a broad range of strike rates. The range of the strike for Figures 3.10 and 3.11 is $[0.033, 0.051]$, which is three standard deviations around the sample mean of 100,000 Monte Carlo samples. We conclude that our trinomial tree can price both caplets and floorlets accurately with a reasonably small number of time steps.

Maturity (year)	Black formula	Tree	Relative difference (%)
0.5	0.000057	0.000058	−0.662214
1.0	0.001650	0.001652	−0.065778
1.5	0.004095	0.004097	−0.053527
2.0	0.006265	0.006267	−0.040104
2.5	0.008020	0.008023	−0.039391
3.0	0.009388	0.009392	−0.036561
3.5	0.010418	0.010422	−0.032941
4.0	0.011160	0.011163	−0.025998
4.5	0.011660	0.011662	−0.015426
5.0	0.011960	0.011960	−0.000591

Table 3.1: Valuation of caplets with strike rate 4.7% and volatility 10% for different maturities. The longest-dated tree $\ln L_{10}$ has 500 time steps

Maturity (year)	Black formula	Tree	Relative difference (%)
0.5	0.000438	0.000440	−0.568200
1.0	0.002474	0.002490	−0.644262
1.5	0.004783	0.004811	−0.585690
2.0	0.006824	0.006866	−0.614040
2.5	0.008503	0.008559	−0.654771
3.0	0.009834	0.009898	−0.643775
3.5	0.010854	0.010918	−0.579240
4.0	0.011608	0.011662	−0.463977
4.5	0.012138	0.012171	−0.270921
5.0	0.012484	0.012484	−0.001922

Table 3.2: Valuation of caplets with strike rate 4.7% and volatility 20% for different maturities. The longest-dated tree $\ln L_{10}$ has 500 time steps

Recall from the previous section that the tree for $\ln L_9$ incurs lower errors in mean and variance than that for $\ln L_1$. Figures 3.12 and 3.13 demonstrate that caplet and floorlet prices for L_9 have smaller relative errors than those of L_1 . Recall also that the tree for $\ln L_{10}$ matches both mean and variance exactly at all nodes. Figures 3.14 and 3.15, respectively, show that caplet and floorlet prices for L_{10} have similar relative errors to those for L_9 . That suggests, at least for our algorithm, the discretization error is as important as, if not more than, the errors in matching the mean and variance.

Maturity (year)	Black formula	Tree	Relative difference (%)
0.5	0.002167	0.002167	−0.011536
1.0	0.000418	0.000419	−0.125781
1.5	0.000106	0.000107	−0.899935
2.0	0.000042	0.000042	−1.184007
2.5	0.000023	0.000024	−1.859791
3.0	0.000016	0.000017	−1.524948
3.5	0.000013	0.000014	−1.493248
4.0	0.000012	0.000013	−1.210493
4.5	0.000012	0.000012	−0.953018
5.0	0.000013	0.000013	−0.473553

Table 3.3: Valuation of floorlets with strike rate 4.7% and volatility 10% for different maturities. The longest-dated tree in L_{10} has 500 time steps

Maturity (year)	Black formula	Tree	Relative difference (%)
0.5	0.002549	0.002550	−0.013684
1.0	0.001250	0.001257	−0.541607
1.5	0.000813	0.000821	−0.923200
2.0	0.000633	0.000641	−1.260881
2.5	0.000550	0.000559	−1.685611
3.0	0.000514	0.000522	−1.677474
3.5	0.000503	0.000510	−1.387797
4.0	0.000505	0.000511	−1.183351
4.5	0.000518	0.000522	−0.680816
5.0	0.000538	0.000538	−0.017919

Table 3.4: Valuation of floorlets with strike rate 4.7% and volatility 20% for different maturities. The longest-dated tree in L_{10} has 500 time steps

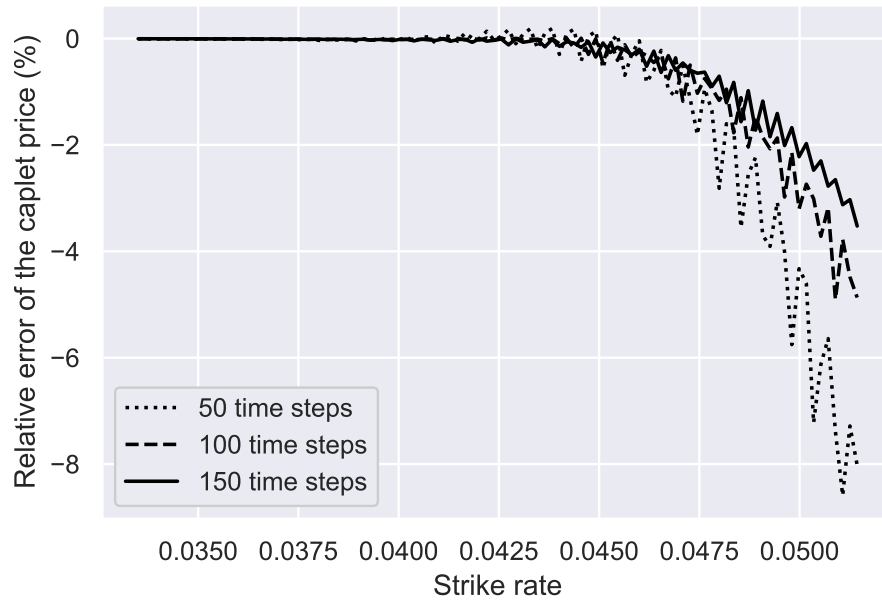


Figure 3.10: Relative errors of caplet prices with maturity 0.5 and volatility 10% against the strike rate.

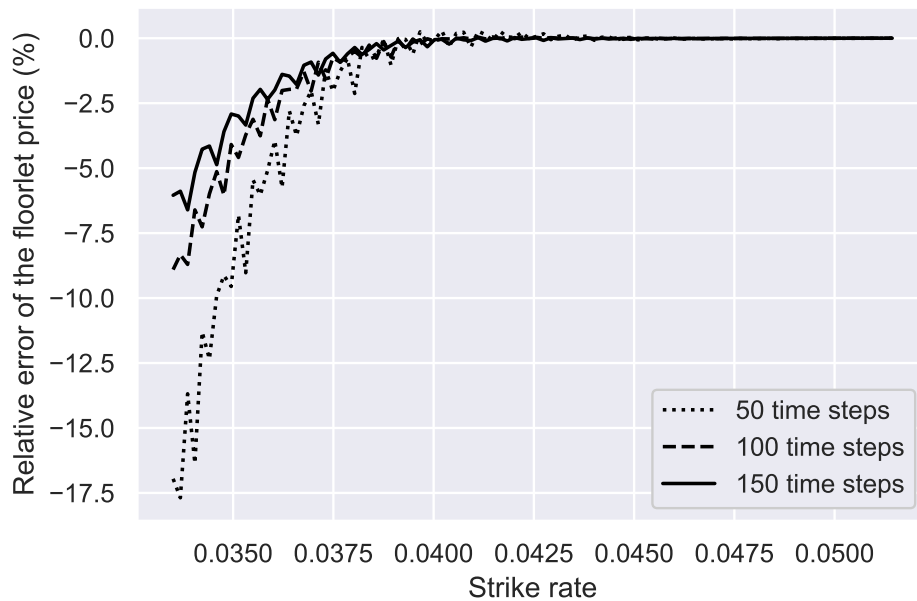


Figure 3.11: Relative errors of floorlet prices with maturity 0.5 and volatility 10% against the strike rate.

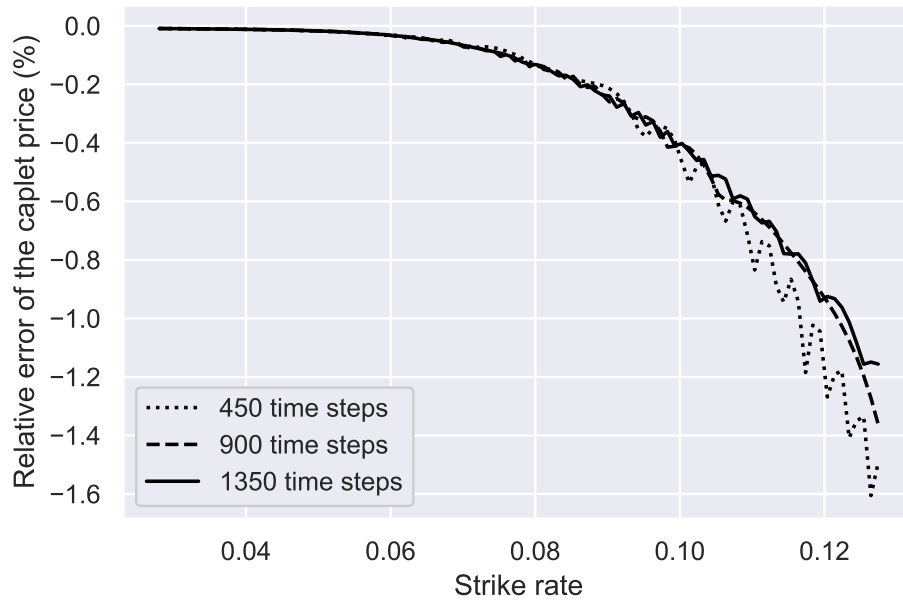


Figure 3.12: Relative errors of caplet prices with maturity 4.5 and volatility 10% against the strike rate.

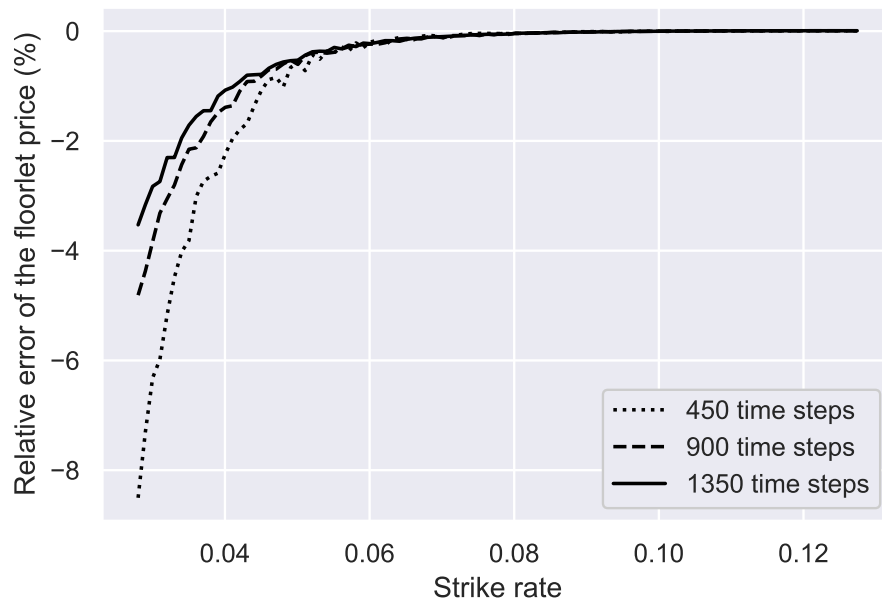


Figure 3.13: Relative errors of floorlet prices with maturity 4.5 and volatility 10% against the strike rate.

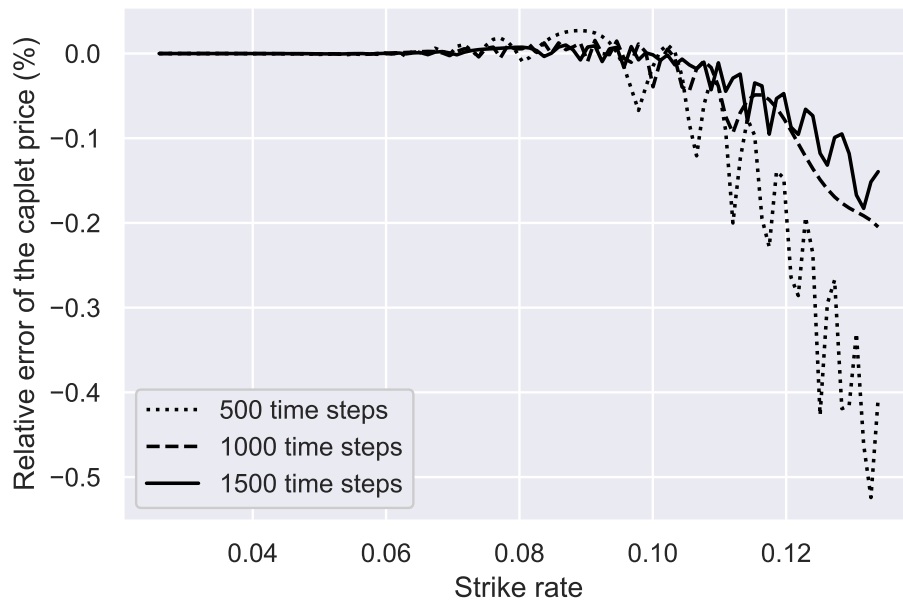


Figure 3.14: Relative errors of caplet prices with maturity 5 and volatility 10% against the strike rate.

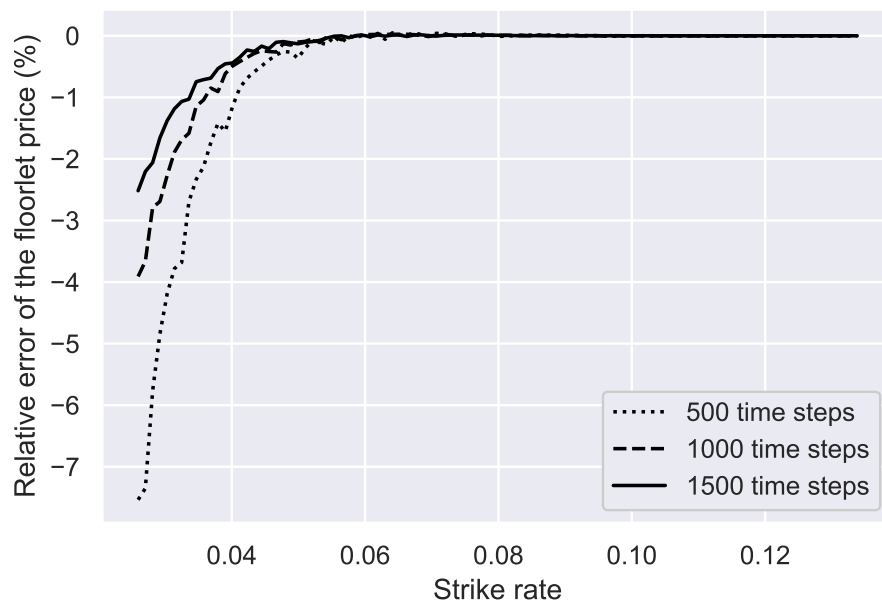


Figure 3.15: Relative errors of floorlet prices with maturity 5 and volatility 10% against the strike rate.

3.3 Valuation of Discrete Barrier Options in the LMM

This section prices discrete barrier options with our trinomial tree. We use the same setup as in the previous section and compare the prices of a discrete up-and-out cap generated by our trinomial tree and those given by Monte Carlo simulation. Specifically, we are modeling four forward LIBOR rates L_1, L_2, L_3 , and L_4 with $T_i = 0.5i$ as the reset date for L_i . We consider a discrete up-and-out cap with strike 4% and barrier 5%. With $\alpha = 0.5$ as the tenor, the payoff at time T_i is $\alpha \cdot \max(L_i(T_{i-1}) - 0.04, 0)$, if $L_k(T_{k-1}) < 0.05$ for all $k \leq i$ and 0 otherwise.

In order to reduce the well-known oscillating convergence of barrier-type options, the trinomial tree has been tilted to match the barrier with one of the terminal nodes (Leisen, 1998). Specifically, for each tree for $\ln L_i$, we find two terminal nodes (N_i, v) and $(N_i, v+1)$ such that $\ln L_i(N_i, v) \leq \ln H \leq \ln L_i(N_i, v+1)$, where H is the barrier rate and N_i is the number of time steps of the tree. We then add a tilt of $u \times [\ln H - \ln L_i(N_i, v)] / N_i$ to each node's value $\ln L_i(u, v)$. This makes the value $\ln L_i(N_i, v)$ in the tilted tree coincide with $\ln H$. Since the distance between adjacent terminal nodes is $O(\sqrt{\Delta t})$, the tilt added to each node only changes the annualized drift by $O(\sqrt{\Delta t})$, which goes to 0 as $\Delta t \rightarrow 0$.

The Monte Carlo price given by Pelsser (2000) with 100,000 samples is 0.003769 with a standard error of 0.000008. Following Tang's (2001) practices, we obtain the 99.99% confidence interval: $[0.003737, 0.003800]$. Figure 3.16 shows that the prices generated by our trinomial tree mostly fall within that confidence interval when it employs more than 1000 time steps.

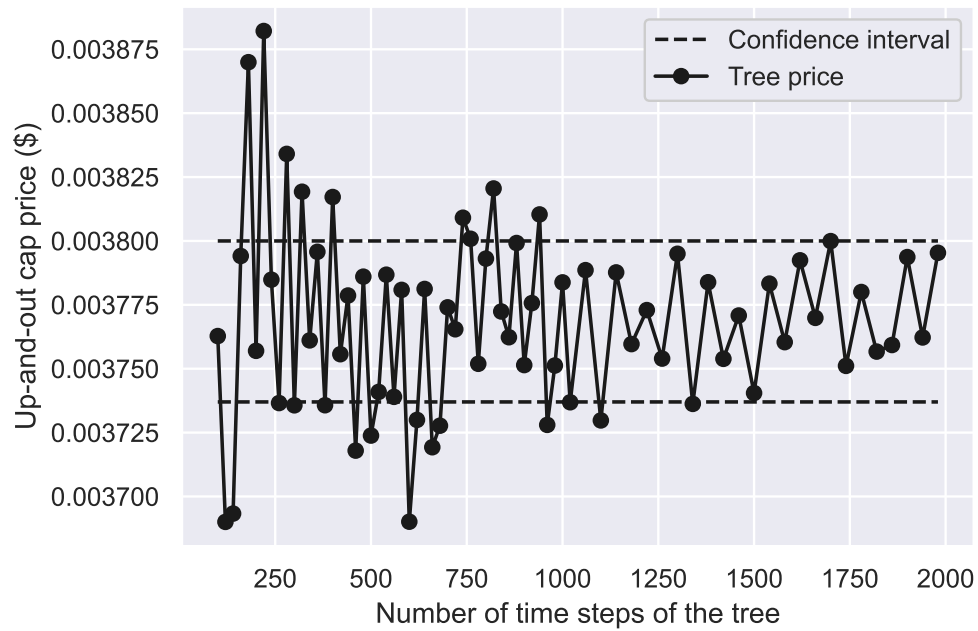


Figure 3.16: Valuation of an up-and-out discrete barrier option with strike rate 4% and barrier rate 5%. The dashed lines denote the bounds of the 99.99% confidence interval generated by the Monte Carlo simulation.

Chapter 4 Conclusion

This thesis proposes a simple quadratic-sized trinomial tree for forward LIBOR rates under the LIBOR market model (LMM). The nodes in the tree are positioned by matching the their means. Although our trinomial tree does not match mean and variance exactly at all nodes, we show numerically that the probability-weighted relative errors for the means and variances of the tree nodes decrease as the number of time steps of the tree increases.

With the trinomial tree, derivatives can be priced by backward induction or forward induction on it. We use our trinomial tree to price caplets, floorlets and discrete barrier options, generating prices very close to the true values.

References

- Black, F. (1976, January). The pricing of commodity contracts. *Journal of Financial Economics*, 3(1–2), 167–179.
- Brace, A., Gatarek, D., & Musiela, M. (1997). The market model of interest rate dynamics. *Mathematical Finance*, 7(2), 127–155.
- Dai, T.-S., Chung, H.-M., & Ho, C.-J. (2009, Dec). Using the libor market model to price the interest rate derivatives: A recombining binomial tree methodology. *NTU Management Review*, 20(1), 41–68.
- Financial Stability Board. (2019). Overnight risk-free rates. a user’s guide. *Financial Stability Board*.
- Gyntelberg, J., & Wooldridge, P. (2008). Interbank rate fixings during the recent turmoil. *BIS Quarterly Review*.
- Harrison, J., & Kreps, D. M. (1979, June). Martingales and arbitrage in multiperiod securities markets. *Journal of Economic Theory*, 20(3), 381–408.
- Ho, T.-S., Stapleton, R. C., & Subrahmanyam, M. G. (1995, October). Multivariate binomial approximations for asset prices with nonstationary variance and covariance characteristics. *Review of Financial Studies*, 8(4), 1125–1152.
- ISDA. (2020). *ISDA launches risk-free rate adoption indicator* (Tech. Rep.). International Swaps and Derivatives Association.
- ISDA. (2023a). *Progress on global transition to RFRs in derivatives markets* (Tech. Rep.). International Swaps and Derivatives Association.
- ISDA. (2023b). *Transition to RFRs review: Full year 2022 and the fourth quarter of 2022* (Tech. Rep.). International Swaps and Derivatives Association.

- Jäckel, P. (2002). *Monte carlo methods in finance*. Chichester, West Sussex, U.K.: Wiley.
- Leisen, D. P. (1998, July). Pricing the American put option: A detailed convergence analysis for binomial models. *Journal of Economic Dynamics and Control*, 22(8-9), 1419–1444.
- Lok, U. H., & Lyuu, Y.-D. (2019, December). Efficient trinomial trees for local-volatility models in pricing double-barrier options. *Journal of Futures Markets*, 40(4), 556–574.
- Lyashenko, A., & Mercurio, F. (2019). Looking forward to backward-looking rates: A modeling framework for term rates replacing LIBOR. *SSRN Electronic Journal*.
- Pelsser, A. (2000). *Efficient methods for valuing interest rate derivatives*. London: Springer.
- Tang, Y., & Lange, J. (2001). A nonexploding bushy tree technique and its application to the multifactor interest rate market model. *Journal of Computational Finance*, 4(4), 5–31.